Zirconium Complexes of a Rigid, Dianionic Pincer Ligand: Alkyl Cations, Arene Coordination, and Ethylene Polymerization

Kelly S. A. Motolko, Jeffrey S. Price, David J. H. Emslie,* Hilary A. Jenkins, and James F. Britten

Department of Chemistry and Chemical Biology, McMaster University, Hamilton, Ontario L8S 4M1, Canada

Supporting Information Placeholder

ABSTRACT: Reaction of H_2XN_2 {4,5-bis(2,4,6-triisopropylanilino)-2,7-di-*tert*-butyl-9,9-dimethylxanthene} with $[Zr(NMe_2)_4]$, followed by crystallization from $O(SiMe_3)_2$, yielded $[(XN_2)Zr(NMe_2)_2]\cdot\{O(SiMe_3)_2\}_{0.5}$ (**1**·$\{O(SiMe_3)_2\}_{0.5}$). The zirconium dimethyl complex $[(XN_2)ZrMe_2]$ (**2**) was subsequently accessed (a) by treatment of **1**·$(O(SiMe_3)_2)_{0.5}$ with excess $AlMe_3$, or (b) via reaction of **1**·$(O(SiMe_3)_2)_{0.5}$ with excess Me_3SiCl, affording $[(XN_2)ZrCl_2]$ (**3**), followed by reaction of **3** with 2 equiv. of MeLi. Reaction of $[(XN_2)ZrMe_2]$ (**2**) with one equiv. of $B(C_6F_5)_3$ or $[CPh_3][B(C_6F_5)_4]$ yielded cationic $[(XN_2)ZrMe][MeB(C_6F_5)_3]$ (**4**) and $[(XN_2)ZrMe(arene)][B(C_6F_5)_4]$ {arene = η^6-benzene (**5a**), η^6-toluene (**5b**), or bromobenzene (**5c**)}, respectively. Both **4** and **5b** are active for ethylene polymerization under 1 atm of ethylene at 24 and 80 °C in toluene, with activities ranging from 23.5–883 kg/(mol·atm·h), yielding polymers with weight-average molecular weights (M_w) of 70,800–88,100 g mol^{-1} and polydispersities (M_w/M_n) of 3.94–4.67.

INTRODUCTION

In combination with a suitable supporting ligand set and weakly-coordinating counteranion, group 4 transition metal alkyl cations may achieve high ethylene polymerization activities, in some cases well in excess of 1000 kg/(mol·atm·h). Highly effective catalysts include metallocenes, *ansa*-metallocenes and constrained geometry catalysts such as $[Cp^*_2ZrMe][A]$, $[\{Me_2Si(\eta^5\text{-9-fluorenyl})(\eta^5\text{-}C_5H_4)\}ZrMe][A]$, and $[\{Me_2Si(\eta^5\text{-}C_5Me_4)(\kappa^1\text{-}N^tBu)\}MMe][A]$ (M = Ti or Zr), as well as non-cyclopentadienyl (post-metallocene) complexes, for example $[(R_3PN)_2TiMe][A]$, $[\{\kappa^2\text{-}CH_2(CH_2NAr)_2\}TiMe][A]$ and $[\{\kappa^2\text{-}OC_6H_2R_2(o\text{-}CH{=}NR)\}_2ZrMe][A]$, where A is a weakly-coordinating anion such as $MeB(C_6F_5)_3$ or $B(C_6F_5)_4$.[1,2,3]

Cationic alkyl complexes are often generated in situ. However, their isolation and characterization can provide valuable insight into the nature of accessible species in solution. Alkyl cations may be categorized as Contact Ion Pairs (CIPs), such as $[Cp^*_2ZrMe][MeB(C_6F_5)_3]$ in which the anion interacts directly with the cation, and Solvent-Separated Ion Pairs (SSIPs), such as $[Cp^*_2ZrMe(THF)][MeB(C_6F_5)_3]$ in which the cation is coordinated by a molecule of solvent and the anion is not present in the primary coordination sphere of the metal.[2] SSIPs in which the metal is coordinated by a donor solvent (e.g. THF, OEt_2 or dme) typically exhibit low or zero polymerization activity, since solvent-coordination diminishes the electrophilicity of the metal centre and increases coordination number, electron count and steric hindrance, reducing the potential for both ethylene coordination and 1,2-insertion. Such SSIPs have been studied in some detail. By contrast, isolated early transition metal and f-element SSIPs incorporating arene solvents are rare (Figure 1),[4,5-7] despite the fact that initial polymerization testing is frequently carried out in arene solvents.[8]

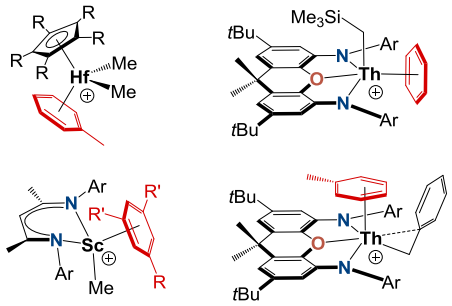

Figure 1. Crystallographically-characterized early transition metal and f-element arene-coordinated alkyl cations (arene-solvent-separated ion pairs). The hafnium complexes were reported by Bochmann {C_5R_5 = 1,3-$C_5H_3(SiMe_3)_2$}[6] and Baird (C_5R_5 = C_5Me_5),[7] and the scandium (R = Me or Br and R' = H, or R = R' = Me)[4] and thorium[5] complexes were reported by Piers and Emslie, respectively (Ar = $C_6H_3{}^iPr_2$-2,6).

The impact of arene-coordination on ethylene polymerization activity is also highly variable. For example, McConville *et al.* proposed arene-coordinated $[\{CH_2(CH_2NAr)_2\}TiR(\eta^6\text{-toluene})]^+$ {Ar = *o*-xylyl or $C_6H_3{}^iPr_2$-2,6} cations to explain greatly reduced polymerization activities in the presence of small amounts of toluene.[9] By contrast, toluene in $[\{t\text{BuN-SiMe}_2(\eta^5,\eta^1\text{-}C_5Me_3CH_2)\}Ti(toluene)][B(C_6F_5)_4]$ is only weakly bound, and this compound is highly active for ethylene (1 atm) polymerization in toluene.[10] Piers also reported the synthesis of $[(\kappa^2\text{-nacnac}^{Me2})ScMe(\eta^6\text{-}C_6R_6)][B(C_6F_5)_4]$

(nacnac^{Me2} = HC(CMeNAr)$_2$; Ar = C$_6$H$_3$^{i}Pr$_2$-2,6; C$_6$R$_6$ = bromobenzene, benzene, toluene, *p*-xylene or mesitylene) scandium cations, and while [(κ^2-nacnac^{Me2})ScMe(η^6-C$_6$H$_3$Me$_3$-1,3,5)][B(C$_6$F$_5$)$_4$] is an active ethylene polymerization catalyst in bromobenzene, it shows negligible activity in more-donating toluene.[4] We also isolated the arene-coordinated thorium cations [(κ^3-XA$_2$)Th(CH$_2$SiMe$_3$)(η^n-arene)][B(C$_6$F$_5$)$_4$] (arene = benzene, *n* = 6; arene = toluene, *n* = 3) and [(κ^3-XA$_2$)Th(*η*^{2}-CH$_2$Ph)(*η*^{6}-toluene)][B(C$_6$F$_5$)$_4$], which are inactive for ethylene (1 atm) polymerization in benzene and toluene solution.[5] Other d^0 arene-solvent-coordinated alkyl cations are: [Cp"MR$_2$(η^6-toluene)][RB(C$_6$F$_5$)$_3$] {M = Zr, R = Me; M = Hf, R = Me or Et; Cp" = 1,3-C$_5$H$_3$(SiMe$_3$)$_2$} in which the arene is tightly coordinated,[6] and [Cp*MMe$_2$(η^6-C$_6$R$_6$)][MeB(C$_6$F$_5$)$_3$] (M = Ti, C$_6$R$_6$ = toluene or mesitylene; M = Zr, C$_6$R$_6$ = benzene, toluene, *p*-xylene, *m*-xylene, mesitylene, styrene; M = Hf, C$_6$R$_6$ = toluene, *p*-xylene, *m*-xylene, mesitylene, styrene, anisole) in which the arene is particularly labile for M = Ti.[7,11]

The complexes discussed above highlight a greater tendency towards arene solvent coordination in more sterically-open cationic alkyl species, especially mono-cyclopentadienyl complexes, and complexes of certain non-cyclopentadienyl ligand systems. We have previously reported a range of actinide and rare earth alkyl complexes supported by 4,5-bis(anilido)xanthene pincer ligands, including complexes of Th,[5,12,13] U,[14] Y,[15] Lu and La.[16] Herein, we report attachment of a rigid, dianionic 4,5-bis(anilido)xanthene pincer ligand (XN$_2$) to zirconium by amine elimination, conversion of the resulting bis(dimethylamido) complex to a dimethyl complex, and subsequent reactions with B(C$_6$F$_5$)$_3$ and [CPh$_3$][B(C$_6$F$_5$)$_4$] to afford a contact ion pair and arene-solvent-separated ion pairs, respectively. The X-ray structures and ethylene polymerization activity of both alkyl cations is discussed.

RESULTS AND DISCUSSION

The amine elimination reaction between H$_2$XN$_2$ {4,5-bis(2,4,6-triisopropylanilino)-2,7-di-*tert*-butyl-9,9-dimethyl-xanthene} and excess [Zr(NMe$_2$)$_4$] (110 °C, 14 days) yielded [(XN$_2$)Zr(NMe$_2$)$_2$]·(O(SiMe$_3$)$_2$)$_{0.5}$ {**1**·(O(SiMe$_3$)$_2$)$_{0.5}$} in 73 % yield after recrystallization from O(SiMe$_3$)$_2$ (Scheme 1). By contrast, reactions of H$_2$XN$_2$ with [M(CH$_2$CMe$_3$)$_4$] (M = Ti or Zr) in benzene led only to a mixture of products including unreacted proligand and [M(CH$_2$CMe$_3$)$_4$] decomposition products at temperatures up to 70 °C. Additionally, [K$_2$(dme)$_x$][XN$_2$] failed to react with MCl$_4$ (M = Ti, Zr or Hf) or MCl$_4$(THF)$_2$ (M = Zr or Hf) in benzene or THF, or ZrI$_4$ in THF, at temperatures up to 90 °C.

Scheme 1. Synthesis of XN$_2$ complex **1** by amine elimination from [Zr(NMe$_2$)$_4$].

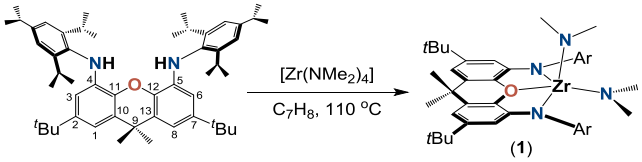

Compound **1**·(O(SiMe$_3$)$_2$)$_{0.5}$ exhibits substantial thermal stability, showing no sign of decomposition after heating at 115 °C in d$_8$-Toluene for 1 week. In the ^{1}H NMR spectrum of **1** at 24 °C, both dimethylamido groups are equivalent. However, de-coalescence was observed upon cooling, resulting in two Zr-N*Me$_2$*, *ortho*-C*H*Me$_2$ and C*Me$_2$* environments at –70 °C. The low-temperature ^{1}H NMR spectrum is indicative of C_s symmetry, presumably with one NMe$_2$ group located approximately in the plane of the ligand, and one in an apical site.

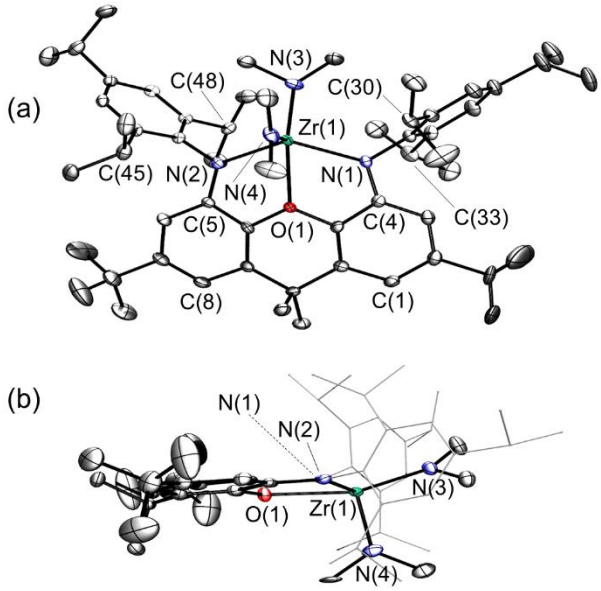

Figure 2. Two views of the X-ray crystal structure for compound **1**. The whole molecule is disordered over two positions, and only the major position (92 %) is shown. Ellipsoids are set to 50 %. Hydrogen atoms are omitted. In view a, the apical NMe$_2$ group points out of the page. In view b, N(1) is located behind N(2), and the 2,4,6-triisopropylphenyl groups are depicted in wire-frame format for clarity. Selected bond lengths [Å] and angles [°]: Zr–N(1) 2.167(4), Zr–N(2) 2.196(4), Zr–N(3) 2.034(5), Zr–N(4) 2.031(5), Zr–O(1) 2.324(4), N(1)–Zr–N(2) 129.2(2), N(1)–Zr–N(3) 103.4(2), N(1)–Zr–N(4) 104.6(2), N(2)–Zr–N(3) 108.5(2), N(2)–Zr–N(4) 106.6(2), N(3)–Zr–N(4) 101.3(2), O(1)–Zr–N(1) 68.2(2), O(1)–Zr–N(2) 67.9(1), O(1)–Zr–N(3) 159.0(2), O(1)–Zr–N(4) 99.4(2).

X-ray quality crystals of **1** were grown from a concentrated O(SiMe$_3$)$_2$ solution cooled to –30 °C (Figure 2), and the solid state structure confirmed that zirconium is 5-coordinate with a distorted square pyramid geometry in which the XN$_2$ ligand donors and one dimethylamido group {N(3)} occupy basal positions, while the second dimethylamido group {N(4)} occupies the axial position. This arrangement of the monodentate ligands mirrors that in structurally-related [(XN$_2$)Ln(CH$_2$SiMe$_3$)(THF)] (Ln = Lu[16] and Y[15]), [Li(THF)$_4$][(XN$_2$)La(CH$_2$SiMe$_3$)$_2$][16] and [(XA$_2$)An(CH$_2$-SiMe$_3$)$_2$] {An = Th and U; XA$_2$ = 4,5-bis(2,6-diisopropyl-anilino)-2,7-di-*tert*-butyl-9,9-dimethyl-xanthene},[12,14] and is favored so as to allow the *N*-aryl groups to rotate away from the apical dimethylamido ligand in order to minimize unfavorable steric interactions. Consequently, the distance between

the isopropyl *C*HMe$_2$ carbon atoms flanking the top of the square pyramid in **1** {C(33)···C(45) = 7.46 Å} is significantly greater than that below the base of the square pyramid {C(30)···C(48) = 5.03 Å}. The square pyramidal coordination geometry of **1** also mirrors that of closely related [(L^{Cy})Ti(NMe$_2$)$_2$] (L^{Cy} = 4,5-dicyclohexyl-2,7-di-*tert*-butyl-9,9-dimethylxanthene), prepared via a salt metathesis reaction between Li$_2$(L^{Cy}) and TiCl$_2$(NMe$_2$)$_2$.[17]

The angles between N(4) and the atoms in the basal plane of **1** range from 99–107°. The smallest angles in the square plane are the N(1)–Zr–O(1) and N(2)–Zr–O(1) angles of 68.2(2) and 67.9(1)°, while the N(1)–Zr–N(3) and N(2)–Zr–N(3) angles are 103.4(2)° and 108.5(2)° respectively, causing the sum of the angles in the square plane to be 348°. The XN$_2$ ligand backbone is slightly bent with a 16° angle between the xanthene aryl rings. Zirconium lies 0.50 Å out of the N(1)/C(4)/C(5)/N(2) plane, leading to a 32° angle between the N(1)/C(4)/C(5)/N(2) and the N(1)/Zr/N(2) planes. The xanthene oxygen donor is located 0.38 Å out of the N(1)/C(4)/C(5)/N(2) plane in order to coordinate to zirconium.

The Zr–N(3) and Zr–N(4) distances of 2.035(5) Å and 2.031(5) Å are in the expected range compared to other zirconium(IV) dimethylamido complexes. For example, the analogous Zr–N distances in [(κ^3-NPN)Zr(NMe$_2$)$_2$] (NPN = PhP{C$_4$H$_n$E(*o*-NAr)}$_2$; E = S, n = 2 Ar = mesityl; E = CH$_2$, n = 4, Ar = *o*-xylyl),[18] [(κ^3-NPN')Zr(NMe$_2$)$_2$] (NPN' = PhP{C$_6$H$_4$(*o*-CH$_2$NAr)}$_2$, Ar = *m*-xylyl),[19] [(κ^3-NNN)Zr(NMe$_2$)$_2$] (NNN = 2,6-NC$_5$H$_3$\{C$_6$H$_4$(*o*-NMes)\}$_2$),[20] [(κ^2-NN)Zr(NMe$_2$)$_2$] [NN = {C$_6$H$_3$(*o*-Me)(*o*-NAr)}$_2$; Ar = C$_6$H$_3$(*m*-^{t}Bu)$_2$],[21] and others[22] range from 2.015(5) Å to 2.086(3) Å. By comparison, the Zr–N(1) and Zr–N(2) distances of 2.167(4) Å and 2.196(4) Å are elongated compared to those for the more electron-donating and less sterically-hindered dimethylamido co-ligands in **1**. However, they are in the typical range for diarylamido ligands; 2.102(5)-2.232(2) Å in the aforementioned Zr complexes.

Reaction of **1**·(O(SiMe$_3$)$_2$)$_{0.5}$ with excess trimethylaluminum in benzene (24 °C, 7 days), afforded [(XN$_2$)ZrMe$_2$] (**2**) as a yellow powder in 62 % yield (Scheme 2). Alternatively, compound **2** could be prepared in two steps via [(XN$_2$)ZrCl$_2$] (**3**). Dichloro compound **3** was isolated in 64 % yield via the reaction of [(XN$_2$)Zr(NMe$_2$)$_2$]·{O(SiMe$_3$)$_2$}$_{0.5}$ (**1**·{O(SiMe$_3$)$_2$}$_{0.5}$) with 2.5 equiv of Me$_3$SiCl in benzene at 24 °C. This reaction required two weeks to reach completion, proceeding via [(XN$_2$)Zr(NMe$_2$)Cl], which was the major product after four days of reaction. Compound **3** was subsequently reacted with excess methyl lithium in C$_6$D$_6$, and the ^{1}H NMR spectrum revealed clean formation of [(XN$_2$)ZrMe$_2$] (**2**).

The difference in thermal stability of **2** compared to **1**·(O(SiMe$_3$)$_2$)$_{0.5}$ is significant, as a d$_8$-toluene solution of **2** was approximately 15 % decomposed after 1 h at 115 °C, and completely decomposed after 18 h.[23] The ^{1}H NMR spectrum of **2** between 24 °C and –70 °C revealed a single peak (0.7 ppm in C$_6$D$_6$ at 24 °C) corresponding to the methyl substituents on zirconium, suggesting either approximate trigonal bipyramidal geometry at zirconium, or a square pyramidal geometry with rapid exchange of the methyl groups in apical and basal positions (*vide infra*).

Scheme 2. Synthesis of dimethyl zirconium complex **2** from bis-amido precursor **1**, directly via reaction with AlMe$_3$, and in 2 steps via dichloro complex **3**.

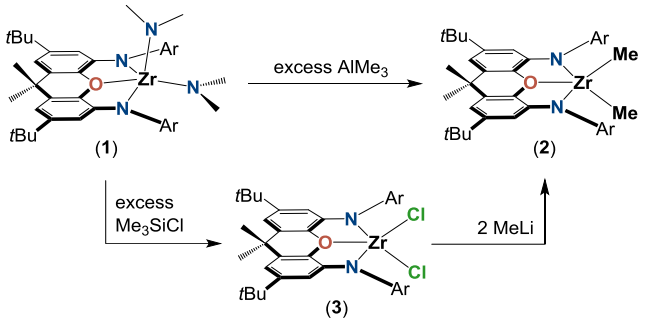

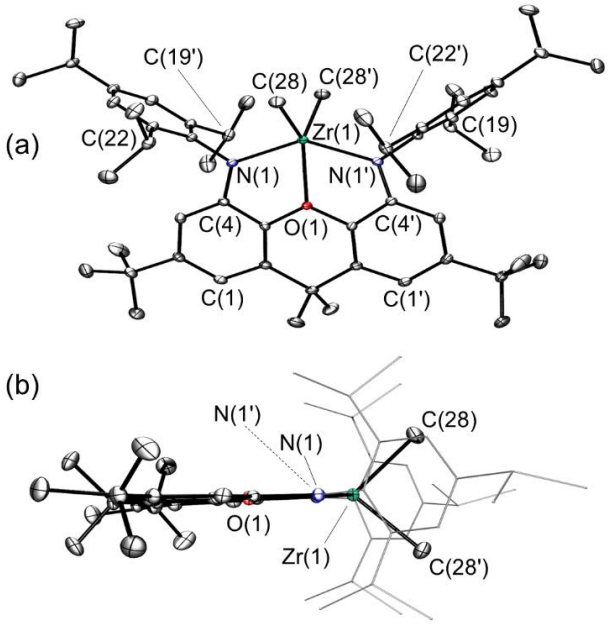

Figure 3. X-ray crystal structure for compound **2**. Ellipsoids are set to 50 %. Hydrogen atoms are omitted for clarity. In view b, the 2,4,6-triisopropylphenyl groups are depicted in wire-frame format for clarity. Selected bond lengths [Å] and angles [°]: Zr–N(1) 2.135(1), Zr–C(28) 2.226(2), Zr–O(1) 2.288(1), N(1)–Zr–N(1') 137.23(7), N(1)–Zr–O(1) 68.62(4), N(1)–Zr–C(28) 104.61(7), O(1)–Zr–C(28) 130.49(6), C(28)–Zr–C(28') 99.0(1).

Crystals of **2** were grown by cooling a concentrated pentane solution to –30 °C (Figure 3), and in contrast to the structure of **1**, compound **2** adopts a distorted trigonal bipyramidal geometry with the amido donors of the XN$_2$ ligand in axial positions; this coordination geometry is likely preferred due to the reduced steric requirements of methyl versus dimethylamido ligands. The N(1)–Zr–N(1') angle is 137.23(7)° due to constraints imposed by ligand rigidity, while the sum of the O–Zr–C(28), O–Zr–C(28') and C(28)–Zr–C(28') angles is exactly 360° due to a C$_2$-axis running through the Zr–O(1) bond. The XN$_2$ ligand is planar, and zirconium lies in the plane of the XN$_2$ ligand donor atoms. The *C*$_2$ axis through the Zr–O(1) bond also leads to identical distances between the *C*HMe$_2$

carbon atoms on either side of the plane of the ligand backbone {C(19)···C(22) = 6.32 Å}.

The Zr–C distances of 2.226(2) Å are comparable with those in complexes such as [(κ^3-^{tBu}NON)ZrMe$_2$] (^{tBu}NON = O{C$_6$H$_4$(N^{t}Bu-*o*)}$_2$) (2.235(5) Å and 2.280(5) Å),[24] [(κ^3-N$_2$NMe)ZrMe$_2$] (N$_2$NMe = (MesNCH$_2$CH$_2$)$_2$NMe; Mes = mesityl) (2.240(7) Å and 2.265(7) Å),[25] and other dimethyl zirconium complexes with bisamido supporting ligands {2.233(6)-2.294(5) Å}.[26] The Zr–N distances of 2.135(1) Å are shorter than the corresponding distances in **1**, perhaps due to reduced steric hindrance. However, they are longer than those in the aforementioned literature compounds {2.087(4)-2.096(4) Å}, apparently due to the large binding pocket of the XN$_2$ ligand enforced by the rigidity of the xanthene backbone.

Scheme 3. Synthesis of methyl zirconium cations **4** and **5a/b**.

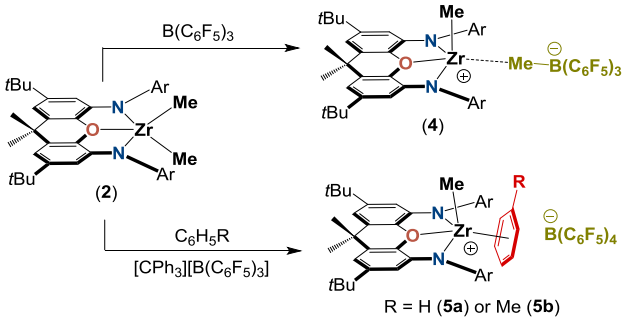

Reaction of **2** with one equivalent of B(C$_6$F$_5$)$_3$ in C$_6$D$_6$ afforded [(XN$_2$)ZrMe][MeB(C$_6$F$_5$)$_3$] (**4**) (Scheme 3), accompanied by an immediate solution colour change from pale yellow to bright golden yellow. Alkyl zirconium cation **4** was isolated as bright yellow crystals in 77 % yield from a concentrated toluene solution layered with pentane and cooled to –30 °C. The ^{1}H NMR spectrum revealed top-bottom asymmetry with two different *ortho*-C*H*Me$_2$ and C*Me$_2$* environments. The Zr-*Me* resonances in the ^{1}H and ^{13}C NMR spectra of **4** (1.87 and 55.56 ppm, respectively) are shifted to high frequency relative to those of neutral [(XN$_2$)ZrMe$_2$] (**2**) (0.78, 50.02 ppm). The B-*Me* signals were observed at 1.80 ppm and 35.20 ppm in the ^{1}H and ^{13}C NMR spectra respectively, and the large chemical shift difference between the *meta*- and *para*-C$_6$F$_5$ signals in the ^{19}F NMR spectrum of **4** {$\Delta\delta$(*m*,*p*-F) = 3.59 ppm} is indicative of a contact ion pair in which the methyl group of the anion interacts significantly with the cation.[27,28] At 24 °C, benzene solutions of [(XN$_2$)ZrMe][MeB(C$_6$F$_5$)$_3$] (**4**) are stable for 24 h. However, after heating a benzene solution of **4** at 60 °C for one hour, 20 % thermal decomposition was observed, and after 18 h, **4** was fully decomposed.[23]

In the solid state structure of **4** (Figure 4), zirconium adopts a distorted square pyramidal geometry with the two amido donors, oxygen, and the methylborate anion {coordinated via C(55)} occupying the square plane, while the remaining methyl ligand {C(54)} caps the pyramid. The smallest angles in the distorted square pyramid are the N–Zr–O angles of 69.18(5) and 69.01(5)°, and the largest is the N(2)–Zr–C(55) angle of 110.97(6)°, while the other angles are between 93° and 105°. The backbone of the XN$_2$ ligand is slightly bent with a 16° angle between the xanthene aryl rings. Zirconium lies 0.32 Å out of the N(1)/C(4)/C(5)/N(2) plane, leading to a 22° angle between the N(1)/C(4)/C(5)/N(2) and the N(1)/Zr/N(2) planes. The neutral oxygen donor of the XN$_2$ ligand is situated 0.36 Å out of the N(1)/C(4)/C(5)/N(2) plane to coordinate to zirconium, and the C(33)···C(45) and C(30)···C(48) distances are 7.61 and 4.82 Å, respectively.

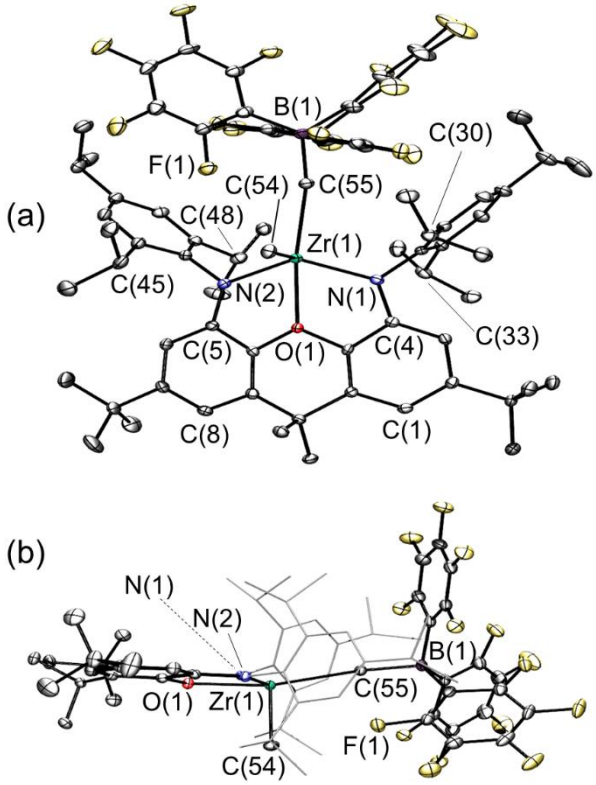

Figure 4. Two views of the X-ray crystal structure for compound **4**·Toluene. Ellipsoids are set to 50 %. Hydrogen atoms and lattice solvent are omitted. In view a, the methyl ligand points out of the page. In view b, N(1) is located behind N(2), and the 2,4,6-triisopropylphenyl groups are depicted in wire-frame format for clarity. Selected bond lengths [Å] and angles [°]: Zr–N(1) 2.093(2), Zr–N(2) 2.093(2), Zr–O(1) 2.254(1), Zr–C(54) 2.207(2), Zr–C(55) 2.560(2), B(1)–C(55) 1.691(3), N(1)–Zr–N(2) 134.32(5), N(1)–Zr–C(54) 100.42(6), N(1)–Zr–C(55) 105.00(6), N(2)–Zr–C(54) 99.03(7), N(2)–Zr–C(55) 110.97(6), C(54)–Zr–C(55) 101.54(7), O(1)–Zr–C(54) 92.59(6), O(1)–Zr–C(55) 165.58(5), O(1)–Zr–N(1) 69.18(5), O(1)–Zr–N(2) 69.01(5).

A range of zirconium alkyl cations paired with a MeB(C$_6$F$_5$)$_3^-$ anion (CIPs) have been reported, with Zr–C$_{Me}$, Zr–C$_{MeBAr3}$ and Me–B distances in the ranges 2.20-2.29 Å, 2.49-2.67 Å and 1.64-1.69 Å, respectively.[24,29,30] The crystal structure of **4** is most closely related to [(^{tBu}NON)ZrMe][MeB(C$_6$F$_5$)$_3$] (^{tBu}NON = O{C$_6$H$_4$(N^{t}Bu-*o*)}$_2$), which features a more flexible dianionic ^{tBu}NON-donor.[24,30] However, a major difference is that the rigid XN$_2$ ligand in **4** is coordinated meridonally, whereas the ^{tBu}NON-donor ligand in [(^{tBu}NON)ZrMe][MeB(C$_6$F$_5$)$_3$] is facially bound; the angle between the N(1)–Zr–O and N(2)–Zr–

O planes is 161° in **4** versus 121° in the ^{tBu}NON complex. The Zr–N distances of 2.093(2) Å in **4** are shorter than those in [(XN_2)ZrMe_2] (**2**) {2.135(1) Å}, consistent with increased Lewis acidity at zirconium, and are equal within error to those in [(^{tBu}NON)ZrMe][MeB(C_6F_5)$_3$] {2.05(1) and 2.07(1) Å}.[24,30]

The Zr–C(54) distance in **4** is 2.207(2) Å, which is only marginally shorter than the Zr–Me distance in neutral [(XN_2)ZrMe_2] (**2**; 2.226(2) Å), and is very similar to that in cationic [(^{tBu}NON)ZrMe][MeB(C_6F_5)$_3$] (2.20(1) Å).[24,30] The Zr–C(55) distance to the methylborate anion is 2.560(2) Å, which is lengthened by 0.35 Å compared to Zr–C(54), and is significantly longer than Zr–C_{MeBAr3} distance in [(^{tBu}NON)ZrMe][MeB(C_6F_5)$_3$] (2.49(1) Å), likely due to increased steric hindrance in the XN_2 compound. However, the Zr–C(55) distance does fall around the middle of the range previously observed for contact ion pairs involving a methyl zirconium cation and a MeB(C_6F_5)$_3$ anion (*vide supra*). The B–C(55) distance of 1.691(3) Å is equal within error to that in [(^{tBu}NON)ZrMe][MeB(C_6F_5)$_3$] {1.69(2) Å}.

Neutral [(XN_2ZrMe_2] (**2**) was also treated with one equivalent of [CPh_3][B(C_6F_5)$_4$] in benzene or toluene, resulting in rapid conversion to [(XN_2)ZrMe(arene)][B(C_6F_5)$_4$] {arene = η^6-benzene (**5a**) or η^6-toluene (**5b**); Scheme 3}, accompanied by a solution colour change from pale yellow to bright red-amber. The ^{1}H NMR spectra of **5a** or **5b** contain two different ortho-C*H*Me_2 and C*Me_2* signals, indicative of C_s symmetry, and cation formation is supported by a shift of the Zr-*Me* ^{1}H NMR resonance to higher frequency; from 0.78 ppm in neutral **2** in C_6D_6 to 0.91 ppm in **5a**.

Crystals of **5b**·(Toluene)$_{0.62}$·(Pentane)$_{1.38}$ were isolated from a concentrated solution of toluene layered with pentane and cooled to –30 °C (Figure 5). Compound **5b** is an arene-solvent-separated ion pair with a toluene molecule π-coordinated to zirconium. The B(C_6F_5)$_4^-$ anion is also located in fairly close proximity to the toluene ligand, with relatively short distances between two fluorine atoms of each of two C_6F_5 rings and the *meta* and *para* carbon atoms of toluene {C(57)–F(4) = 3.114 Å, C(57)–F(5) 3.103 Å, C(58)–F(5) 3.052 Å, C(58)–F(6) 3.358 Å, C(59)–F(7) 3.131 Å}.

The three anionic donors, O(1), and the centroid of aromatic ring of toluene can be considered to form either a distorted square pyramid with C(54) in the apical site, or an edge-capped tetrahedron with O(1) capping the N(1)–N(2) edge. The N–Zr–C(54) angles are 99.3(2) and 99.5(2)°, the N(1)–Zr–N(2) angle is 132.3(2)°, and the E–Zr–Cent {E = N(1), N(2) or C(54); Cent = the C_6H_5Me ring centroid} angles are between 105° and 109°. Additionally, the N–Zr–O angles are 70.1(1) and 70.2(1)°, the C(54)-Zr–O(1) angle is 81.0(2)°, and the O–Zr–Cent angle is 174°. The XN_2 ligand backbone is slightly bent with a 19° angle between the xanthene aryl rings.

Zirconium lies 0.52 Å out of the N(1)/C(4)/C(5)/N(2) plane, leading to a 37° angle between the N(1)/C(4)/C(5)/N(2) plane and the N(1)/Zr/N(2) plane. This distance and angle are significantly larger than those in **4** (0.32 Å and 22°), indicative of increased steric hindrance in **5b** compared to **4** as a result of toluene rather methylborate coordination. The difference in the distances between the isopropyl *C*HMe_2 carbon atoms on either side of the plane of the xanthene backbone is also larger in **5b** than in **4**; 3.25 vs 2.79 Å {in **5b**, C(33)···C(48) = 7.79 Å and C(30)···C(45) = 4.54 Å}. However the neutral oxygen donor of the XN_2 ligand is situated 0.36 Å out of the N(1)/C(4)/C(5)/N(2) plane in both **4** and **5b**.

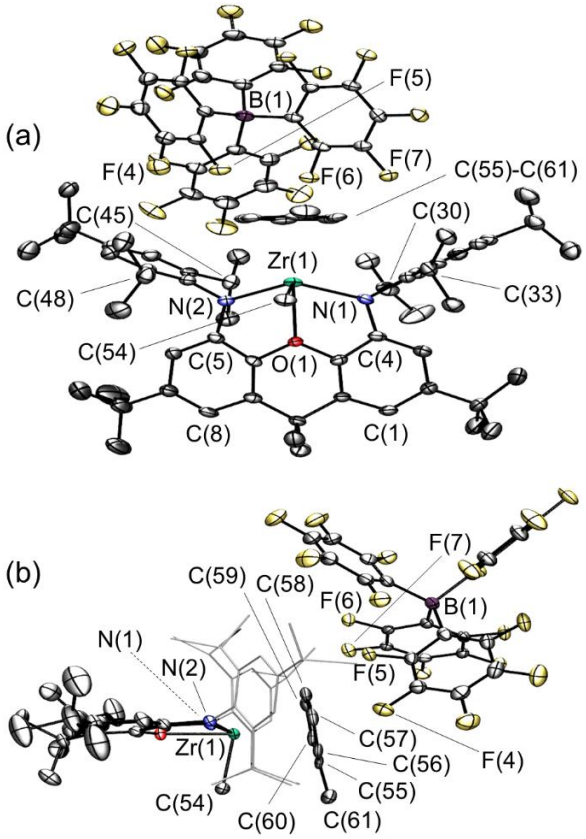

Figure 5. Two views of the X-ray crystal structure for compound **5b**·(Toluene)$_{0.62}$·(Pentane)$_{1.38}$. Ellipsoids are set to 50 %. Hydrogen atoms and lattice solvent are omitted. In view a, the methyl ligand points out of the page. In view b, N(1) is located behind N(2), and the 2,4,6-triisopropylphenyl groups are depicted in wire-frame format for clarity. Selected bond lengths[Å] and angles [°]: Zr–N(1) 2.142(4), Zr–N(2) 2.138(4), Zr–O(1) 2.220(3), Zr–C(54) 2.239(5), Zr–C(55) 2.841(5), Zr–C(56) 2.789(5), Zr–C(57) 2.766(5), Zr–C(58) 2.706(5), Zr–C(59) 2.696(5), Zr–C(60) 2.746(5), N(1)–Zr–N(2) 132.3(2), N(1)–Zr–C(54) 99.5(2), N(2)–Zr–C(54) 99.3(2), O(1)–Zr–C(54) 81.0(2), O(1)–Zr–N(1) 70.1(1), O(1)–Zr–N(2) 70.2(1).

The Zr–C(54) {2.239(5) Å} and Zr–N {2.142(4), 2.138(4) Å} bonds in **5b** are slightly longer than those in **4** {Zr–C(54) = 2.207(2) Å; Zr–N = 2.093(2), 2.093(2) Å}, perhaps as a consequence of increased steric hindrance. However, the Zr–O distance in cation **5b** is marginally shorter than that in **4** {2.220(3) vs 2.254(1) Å}, and the Zr–C_{alkyl}, Zr–N and Zr–O distances in **5b** are otherwise unremarkable. The Zr–C_{arene} distances range from 2.706(5) (*para*) to 2.696(5)-2.789(5) (*ortho* and *meta*) and 2.841(5) Å (*ipso*), all of which are well within the sum of the van der Waals radii (3.9-4.3 Å),[31] consistent with η^6-coordination {Zr–C_{arene} (ave.) = 2.76 Å}.

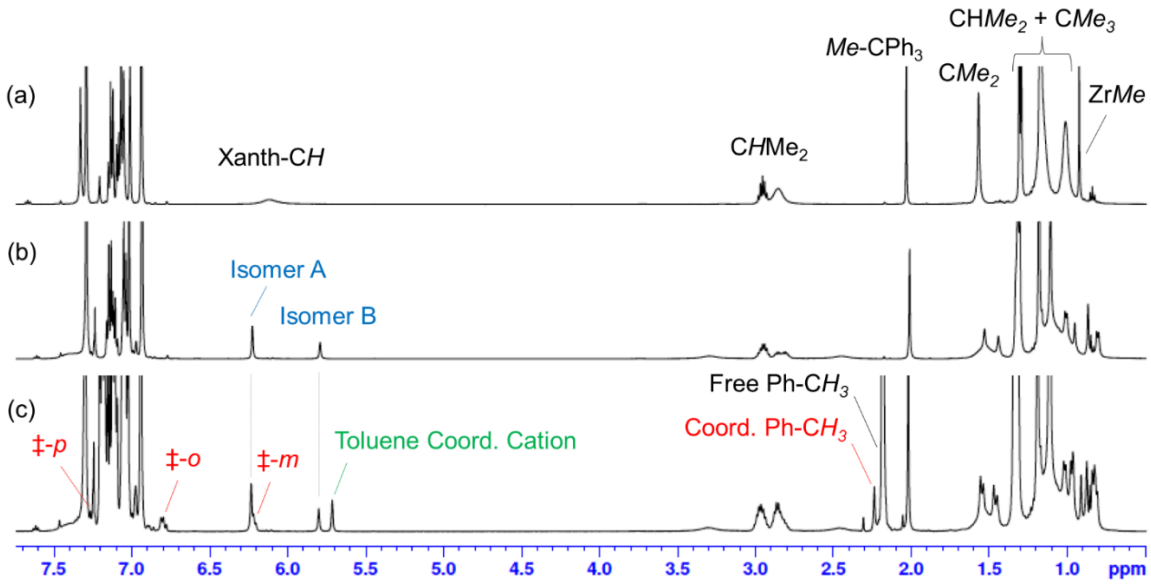

Figure 6. ^{1}H NMR spectra of [(XN$_2$)ZrMe(arene)][B(C$_6$F$_5$)$_4$] (**5**; arene = C$_6$D$_5$Br or η^6-C$_6$H$_5$Me) generated in-situ via the reaction of [(XN$_2$ZrMe$_2$] (**2**) with one equivalent of [CPh$_3$][B(C$_6$F$_5$)$_4$] in *d*$_5$-bromobenzene, (a) at 25 °C, (b) at –25 °C, and (c) at –25 °C after addition of 10 equiv. of toluene. Isomers A and B are isomers of [(XN$_2$)ZrMe(C$_6$D$_5$Br)][B(C$_6$F$_5$)$_4$].

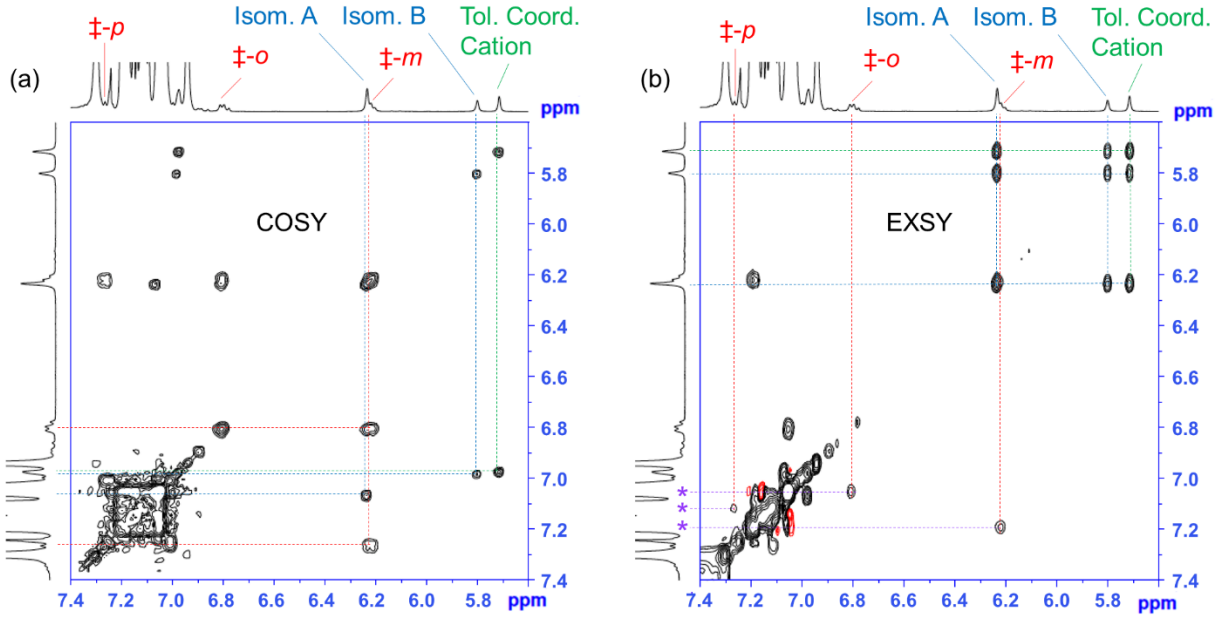

Figure 7. Selected regions of the –25 °C 2D-COSY (a) and 2D-EXSY (b) NMR spectra of [(XN$_2$)ZrMe(arene)][B(C$_6$F$_5$)$_4$] (**5**; arene = C$_6$D$_5$Br and η^6-C$_6$H$_5$Me) generated in-situ in *d*$_5$-bromobenzene, followed by addition of 10 equiv. of toluene. * = C$_6$*H*$_5$Me peaks of free toluene. ‡ = C$_6$*H*$_5$Me peaks of coordinated toluene. Isomers A and B are isomers of [(XN$_2$)ZrMe(C$_6$D$_5$Br)][B(C$_6$F$_5$)$_4$].

Complex **5b** is the first crystallographically-characterized example of an arene-solvent-coordinated zirconium alkyl cation. The M–C$_{arene}$ distances in **5b** are longer, on average, than those in [(C$_5$R$_5$)HfMe$_2$(η^6-toluene)] {C$_5$R$_5$ = C$_5$H$_3$(SiMe$_3$)$_2$-1,3 and C$_5$Me$_5$; Figure 1} which range from 2.62 to 2.81 Å {Zr–C$_{arene}$ (ave.) = 2.69 Å}. The structure of **5b** is also similar to that of [(XA$_2$)Th(CH$_2$SiMe$_3$)(η^6-C$_6$H$_6$)] (Figure 1),[5] although the M–C$_{arene}$ distances in the thorium complex range from 3.21 to 3.31 Å, suggestive of a significantly weaker metal–arene interaction, given that the difference in the ionic radii of thorium(IV) and zirconium(IV) is 0.22 Å.[32]

After removal of supernatant from crystals of **5b**, the solid is stable for very short periods of time under argon. However, after 10 min under argon in the glovebox or after exposure to vacuum, ^{1}H NMR spectroscopy showed extensive decomposition to unidentified products. Presumably, coordinated toluene in **5b** readily dissociates, and in the absence of other stabilizing donor ligands, decomposition ensues. By contrast, in solu-

tion in d_8-toluene, cation **5b** is thermally stable at 24 °C, and minimal decomposition was observed after 18 h at 60 °C. However, 50 % decomposition was evident after 18h at 80 °C, and decomposition was complete after 48h at this temperature.[23] The solution stability of **5b** contrasts that of **4**, which was fully decomposed after 18 h at 60 °C (*vide supra*), suggesting that toluene coordination in **5b** contributes significantly to the stability of the complex.

Bromobenzene-coordinated $[(XN_2)ZrMe(C_6D_5Br)][B(C_6F_5)_4]$ (**5c**) was also generated *via* the 1:1 reaction of **2** with $[CPh_3][B(C_6F_5)_4]$ in C_6D_5Br, and the resulting cation, $[(XN_2)ZrMe(C_6D_5Br)][B(C_6F_5)_4]$ (**5c**) exists as a 1:0.53 mixture of isomers in solution. These isomers do not appear to involve $B(C_6F_5)_4$ anion coordination, since addition of 2 equiv. of $[NBu_4][B(C_6F_5)_4]$ did not change the ratio of the two isomers, nor did it give rise to a new set of ^{19}F NMR signals or significantly alter the ^{19}F NMR chemical shifts for the $B(C_6F_5)_4$ anion. Therefore, the two isomers of **5c** are likely a κ^1*Br*-coordinated and a π-coordinated isomer (isomers A and B; Figure 8).[33]

At room temperature, the two isomers are in rapid exchange, but at –25 °C, a distinct set of xanthene $CH^{1/8}$ and $CH^{3/6}$ peaks was observed for each isomer (a and b in Figure 6). Addition of 6 equiv of toluene to a solution of **5c** in C_6D_5Br afforded a ^1H NMR spectrum (–25 °C) with a new set of signals for toluene-coordinated **5b** in addition those for **5c** (both isomers) in a 0.26:1 ratio, which increased to 0.44:1 upon introduction of 4 further equiv of toluene (c in Figure 6). A –20 °C 2D-EXSY NMR spectrum (b in Figure 7) revealed that **5b** and both isomers of **5c** are in equilibrium with one another. Furthermore, signals for coordinated toluene were observed at 7.26, 6.80, 6.21 and 2.23 ppm (C*H*-*p*, C*H*-*o*, C*H*-*m* and CH_3, respectively), with COSY peaks between the *meta* and the *ortho* and *para* positions, and EXSY correlations between all four coordinated toluene signals and free toluene (a and b in Figure 7).

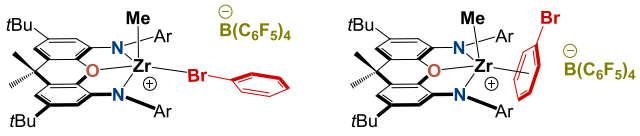

Figure 8. Plausible structures for isomers A and B of $[(XN_2)ZrMe(bromobenzene)][B(C_6F_5)_4]$ (**5c**).

The behaviour of **5b** in C_6D_5Br contrasts that of the thorium analogue, $[(XA_2)Th(CH_2SiMe_3)(\eta^6\text{-toluene})]$, which exhibits sharp peaks due to free (6 equiv.) and coordinated toluene (6.92, 6.67, 5.91, 2.02 ppm for the C*H*-*p*, C*H*-*o*, C*H*-*m* and CH_3 signals, respectively) in the room temperature ^1H NMR spectrum, and is not in equilibrium with a noticeable amount of a bromobenzene-coordinated cation.[5] The greater lability of toluene in **5b** is surprising given that the average M–C_{arene} distances in the solid state structure of **5b** are significantly shorter than those in the thorium cation, even after taking into account differences in metal ionic radius.

Cations **4** and **5a** (generated in situ in C_6D_6) were evaluated as catalysts for intramolecular hydroamination utilizing 1-amino-2,2-diphenyl-4-pentene with 10 mol % catalyst loading at 24 °C, resulting in very slow conversion to the product (55 % and 95 % complete for **4** and **5a** respectively after 17 days). Due to the low activity of **4** and **5a** for cyclization of 1-amino-2,2-diphenyl-4-pentene, which is considered to be one of the most readily cyclized substrates, further testing was not pursued. Neutral **2** was also assessed as a catalyst for intramolecular hydroamination utilizing 1-amino-2,2-diphenyl-4-pentene under the same conditions (10 mol %, 24 °C in C_6D_6) affording negligible conversion after 2 weeks. However, with the same substrate, heating **2** (10 mol %, 110 °C in d_8-Toluene) gave 10 % conversion after 24 hours, and >99 % after 7 days.

Both $[(XN_2)ZrMe][MeB(C_6F_5)_3]$ (**4**) and $[(XN_2)ZrMe(\eta^6\text{-toluene})][B(C_6F_5)_4]$ (**5b**) are active ethylene polymerization catalysts at 24 °C and 80 °C (~ 1.2 mM catalyst in toluene) under 1 atm of ethylene, and catalytic activities and polymer properties are summarized in Table 1. Compound **4** showed a moderate activity of 23.5 kg/(mol·atm·h) after 30 min at 24 °C, while **5b** achieved high activities of 273 kg/(mol·atm·h) after 30 min and 883 kg/(mol·atm·h) after 5 min at 24 °C. At 80 °C (30 min), the activity of **4** increased to 118 kg/(mol·atm·h), whereas that of **5b** decreased to 113 kg/(mol·atm·h), despite the fact that **5b** was found to be more thermally stable than **4** in toluene at 80 °C (*vide supra*).

Table 1: Ethylene polymerization data for catalysts **4** and **5** (1.2 mM concentration) under 1 atm of ethylene. The catalyst is generated *in situ* by reaction of $[(XN_2)ZrMe_2]$ (**2**) with 1 equiv. of activator in arene solvent (toluene unless otherwise specified).

Activator[a]	Temp. (°C)	Time (min)	Yield (g)	Activity (kg/(mol·atm·h)	M_w (g/mol)[b]	M_w/M_n[b]	T_m (°C)[c]
BAr_3	24	30	0.067	23.5	–[e]	–[e]	125.8
BAr_3	80	30	0.338	118	70 800	3.94	121.0
CPh_3^+	24	30	0.778	273	78 300	4.66	124.6
CPh_3^+	24	5	0.418	883	88 100	4.65	123.0
CPh_3^+	80	30	0.322	113	81 900	4.67	123.2
CPh_3^+	24[d]	2[d]	0.057[d]	300	52 200	3.30	124.4

(a) $BAr_3 = B(C_6F_5)_3$; $[CPh_3]^+ = [CPh_3][B(C_6F_5)_4]$. (b) GPC is relative to polystyrene standards, and M_w and M_w/M_n values are averages from two duplicate GPC runs. (c) Peak melting temperature, T_m, from DSC (2nd heating run). (d) In-situ catalyst generation and polymerization was carried out in bromobenzene. (e) The polymer was insoluble in 1,2,4-trichlorobenzene at 140 °C, and therefore was not amenable to analysis by GPC.

The decreased activity of **5b** after 30 min *vs* 5 min at 24 °C is likely due to ensnarement of the catalyst in precipitated polyethylene, given that the catalyst maintains some activity at 80 °C. Nevertheless, the decreased activity of **5b** at 80 vs 24 °C is presumably an indication of significant catalyst decomposition at 80 °C, highlighting the important role of the anion in stabilizing cationic species involved in catalysis. The apparent discrepancy in the relative thermal stabilities of **4** and **5b**

alone vs in the presence of ethylene at 80 °C can be attributed to differences in the solution species present under these conditions, including ethylene-coordinated and β-hydrogen-containing alkyl cations formed during polymerization.

Polyethylene generated by **4** or **5b** in toluene has a fairly high polystyrene equivalent weight-average molecular weight (M_w = 70,800-88,100 g/mol) with a relatively high polydispersity (M_w/M_n) of 3.94 for cation **4** (80 °C) and 4.65-4.67 for cation **5b** (24 and 80 °C). By contrast, cation **5c** generated in bromobenzene (24 °C, 2 min) yielded a lower molecular weight polymer (52,200 g/mol) with a somewhat narrower polydispersity (3.30), compared to the closely analogous reaction in toluene (Table 1). Polyethylene generated by **4** at 24 °C had the highest DSC peak melting temperature (T_m = 125.8 °C vs 121.0-124.6 °C for all other samples), and was insufficiently soluble in 1,2,4-trichlorobenzene at 140 °C for GPC, suggestive of a higher molecular weight polymer. However, all of the observed T_m values are lower than those typically observed for polyethylene with similar M_w values, perhaps indicative of appreciable chain branching.

The ethylene polymerization activity of **5b/c** compares well with that of other non-cyclopentadienyl zirconium catalysts. For example: (a) [(κ^3-$^{t\mathrm{Bu}}$NON)ZrMe][MeB(C_6F_5)$_3$] afforded an activity of ~100 kg/(mol·atm·h) under 1-2 atm ethylene (22 °C, 2 min),[30] (b) [(κ^2-NN')ZrMe$_2$] {NN' = $CH_2(CH_2NSi^iPr_3)_2$} achieved an activity of 1.5 kg/(mol·atm·h) after activation with B(C_6F_5)$_3$ and 317 kg/(mol·atm·h) after activation with [CPh_3][B(C_6F_5)$_4$] at 24 °C (1 atm of ethylene, 1h),[27] and (c) [(κ^2-NN")ZrMe$_2$] / B(C_6F_5)$_3$ (NN" = {CH_2(*o*-C_6H_4)NSi^iPr_3}$_2$) yielded an activity of 178 kg/(mol·atm·h) after 5 min at 0 °C under 1 atm of ethylene, affording a M_w value of 165 kg/mol and a PDi (M_w/M_n) of 1.96.[34] By contrast, [(κ^3-NNN')ZrMe$_2$] (NNN' = NC_5H_3(*o*-CHAr–NAr')(*o*-X); X = 2-pyrrolyl or 2-indolyl; Ar = $C_6H_4{}^i$Pr-2; Ar' = $C_6H_3{}^i$Pr$_2$-2,6} achieved no more than trace activity under 1 atm of ethylene at 25 °C after activation with B(C_6F_5)$_3$ or [CPh_3][B(C_6F_5)$_4$].[35] Nevertheless, substantially higher activities have been reported for some homogeneous zirconium catalyst systems, such as [(κ^3-Tp$^{\mathrm{Ms*}}$)ZrCl$_3$]/MAO {Tp$^{\mathrm{Ms*}}$ = HB(3-mesitylpyrazolyl)$_2$(5-mesitylpyrazolyl)}[36] and [(κ^2-L)$_2$ZrCl$_2$]/MAO {L = salicylaldiminate = OC_6H_2(2-CH=NCy)(4-Me)(6-CMe_2Ph)}.[3]

SUMMARY AND CONCLUSIONS

Attempts to coordinate the XN_2 ligand to zirconium via salt metathesis or alkane elimination were unsuccessful. However, XN_2 ligand attachment was achieved through the amine elimination reaction between H_2XN_2 and [Zr(NMe_2)$_4$], forming [(XN_2)Zr(NMe_2)$_2$]·($O(SiMe_3)_2$)$_{0.5}$ (**1**·($O(SiMe_3)_2$)$_{0.5}$). Compound **1** served as the entry point for the synthesis of [(XN_2)ZrCl_2] (**3**) and [(XN_2)ZrMe_2] (**2**), and reactions of **2** with B(C_6F_5)$_3$ and [CPh_3][B(C_6F_5)$_4$] afforded the alkyl cations [(XN_2)ZrMe][MeB(C_6F_5)$_3$] (**4**) and [(XN_2)ZrMe(arene)]-[B(C_6F_5)$_4$] {arene = η^6-benzene (**5a**), η^6-toluene (**5b**), and bromobenzene (**5c**)}. Compound **4** is a contact ion pair whereas **5b** is a rare example of an arene-solvent-separated ion pair, and both highlight the ability of rigid 4,5-bis(anilido)xanthene ligands such as XN_2 to stabilize highly-reactive organometallic species. In bromobenzene containing 10 equiv. of toluene, a 0.44:1 mixture of **5b**:**5c** is observed. At –25 °C, bromobenzene-coordinated **5c** exists as a mixture of two isomers (likely η^6-coordinated and a κ^1-*Br*-coordinated cations), and all three solution species (**5b** and both isomers of **5c**) are in rapid exchange at room temperature. Compounds **4** and **5b/c** are moderately to highly active for ethylene polymerization at 24 or 80 °C under 1 atm. of ethylene {max. 883 kg/(mol·atm·h)}, yielding polymers with weight-average molecular weights of 52,200–88,100 g/mol and polydispersities of 3.30–4.67 across all soluble samples.

EXPERIMENTAL SECTION

General Details:

An argon-filled MBraun UNIlab glove box equipped with a –30 °C freezer was employed for the manipulation and storage of all air-sensitive compounds, and reactions were performed on a double manifold high vacuum line using standard techniques.[37] A Fisher Scientific Ultrasonic FS-30 bath was used to sonicate reaction mixtures where indicated. Commonly utilized specialty glassware includes the swivel frit assembly, J-Young NMR tubes, and thick walled flasks equipped with Teflon stopcocks.

Diethyl ether (Et_2O), tetrahydrofuran (THF), toluene, benzene and hexanes were initially dried and distilled at atmospheric pressure from Na/Ph_2CO. Hexamethyldisiloxane ($O(SiMe_3)_2$) was dried and distilled at atmospheric pressure from Na. Unless otherwise noted, all proteo solvents were stored over an appropriate drying agent (pentane, hexanes, hexamethyldisiloxane ($O(TMS)_2$ / $O(SiMe_3)_2$) = Na/Ph_2CO/tetra-glyme; Et_2O, 1,2-dimethoxyethane (DME), THF, toluene, benzene = Na/Ph_2CO) and introduced to reactions via vacuum transfer with condensation at –78 °C. The deuterated solvents (ACP Chemicals) C_6D_6, THF-d_8 and toluene-d_8 were dried over Na/Ph_2CO. The H_2XN_2 ligand,[15] and the intramolecular hydroamination reagents[38] were prepared according to literature procedures. MeLi (1.6 M in Et_2O) and Me_3SiCl were purchased from Sigma-Aldrich. Solid MeLi was obtained by removal of solvent *in vacuo*. [Zr(NMe_2)$_4$], $AlMe_3$ and trityltetrakis(pentafluorophenyl)borate were purchased from Strem Chemicals. [Zr(NMe_2)$_4$] was sublimed prior to use. C_6F_5Br (used for the synthesis of B(C_6F_5)$_3$ was purchased from Oakwood Chemicals and distilled from molecular sieves prior to use. B(C_6F_5)$_3$ was prepared from C_6F_5MgBr and $BF_3(OEt_2)$ according to the literature procedure.[39] Argon (99.999 % purity) and ethylene (99.999 % purity) were purchased from Praxair, and both were passed through an Oxisorb-W scrubber from Matheson Gas Products, in order to remove residual oxygen and moisture.

Combustion elemental analyses were performed by Midwest Microlab, LLC, Indianapolis, Indiana. A VWR Clinical 200 Large Capacity Centrifuge (with 28° fixed-angle rotors that hold 12 × 15 mL or 6 × 50 mL tubes) in combination with 15 mL Kimble Chase glass centrifuge tubes was used when required (inside the glovebox). NMR spectroscopy (^{1}H, ^{13}C{^{1}H}, ^{19}F, DEPT-Q, COSY, HSQC, HMBC) was performed on Bruker AV-200, DRX-500 and AV-600 spectrometers. All ^{1}H NMR and ^{13}C NMR spectra were referenced relative to $SiMe_4$ through a resonance of the employed deuterated solvent or proteo impurity of the solvent; C_6D_6 (7.16 ppm), d_8-Tol (2.08, 6.97, 7.01, 7.09 ppm), d_8-THF (1.72, 3.58 ppm) for ^{1}H NMR; and C_6D_6 (128.0 ppm), d_8-Tol (20.43, 125.13, 127.96, 128.87, 137.48 ppm), d_8-THF (25.31, 67.21 ppm) for ^{13}C NMR. ^{19}F NMR spectra were referenced using an external standard of $CFCl_3$ (0.0 ppm). Herein, numbered proton and carbon atoms refer to the positions of the xanthene backbone, as shown in Scheme 1. Inequivalent ortho isopropyl protons are labeled A and B, while inequivalent aryl ring protons and inequivalent methyl protons are labeled ' and ", so that the corresponding carbon resonances can be identified. X-ray crystallographic analyses were performed on suitable crystals coated in Paratone oil and mounted on a SMART APEX II diffractometer with a 3 kW Sealed tube Mo generator in the McMaster Analytical X-

Ray (MAX) Diffraction Facility. In all cases, non-hydrogen atoms were refined anisotropically and hydrogen atoms were generated in ideal positions and then updated with each cycle of refinement.

All GPC data were recorded on an Agilent PL220 high temperature instrument equipped with differential refractive index (DRI) and viscometry (VS) detectors at the University of Warwick, Coventry, UK by Dr. D. W. Lester and Dr. I. Hancox. The system was equipped with 2 × PLgel Mixed D columns (300 × 7.5 mm) and a PLgel 5 μm guard column. Samples were dissolved in TCB (trichlorobenzene) and left to solubilise for 12 hours on an Agilent PL SP260VS at 140 °C and all data was calibrated against polystyrene. The mobile phase was TCB stabilised with 250 ppm BHT and run at a flow rate of 1 mL/min at 160 °C. Thermal properties of PE samples were investigated by DSC (TA Instruments DSC Q20) between 40 and 160-180 °C using a heating and cooling rate 10 °C min^{-1}; peak melting temperatures were obtained from the second of two heating runs.

[(XN$_2$)Zr(NMe$_2$)$_2$]·(O(SiMe$_3$)$_2$)$_{0.5}$ (1·(O(SiMe$_3$)$_2$)$_{0.5}$): H_2XN_2 (1.5 g, 1.98 mmol) was dissolved in 14 mL of toluene and added to [Zr(NMe$_2$)$_4$] (1.58 g, 5.94 mmol) which was then stirred at 110 °C in a sealed Schlenk flask for 14 days. The solvent was removed *in vacuo* and the brown solid was heated at 90 °C to remove excess [Zr(NMe$_2$)$_4$] by sublimation. The remaining product was recrystalized from O(SiMe$_3$)$_2$ at –30 °C yielding **1**·(O(SiMe$_3$)$_2$)$_{0.5}$ as a brown solid (1.46 g, 73 %). **^{1}H NMR (C$_6$D$_6$, 600 MHz):** δ 7.28 (s, 4H, Ar-*H*), 6.82 (d, 2H, $^4J_{H,H}$ 1.96 Hz, Xanth-C*H*^{1}), 6.25 (d, 2H, $^4J_{H,H}$ 1.96 Hz, Xanth-C*H*^{3}), 3.57 (sept, 4H, $^3J_{H,H}$ 6.86 Hz, ortho-C*H*Me$_2$), 2.88 (sept, 2H, $^3J_{H,H}$ 6.86 Hz, para-C*H*Me$_2$), 2.62 (br. s, 12H, Zr(N*Me$_2$*)$_2$), 1.60 (s, 6H, C*Me$_2$*), 1.30 (d, 12H, $^3J_{H,H}$ 6.86 Hz, A-ortho-CH*Me$_2$*), 1.26 (d, 12H, $^3J_{H,H}$ 6.86 Hz, para-CH*Me$_2$*), 1.25 (d, 12H, $^3J_{H,H}$ 6.86 Hz, B-ortho-CH*Me$_2$*), 1.24 (s, 18H, C*Me$_3$*). **^{13}C NMR (C$_6$D$_6$, 126 MHz):** δ 148.13 (Xanth-*C*^{2}), 147.17 (Xanth-*C*^{4}), 146.36 (para-*C*CHMe$_2$), 146.26 (ortho-*C*CHMe$_2$), 140.86 (Ar-*C*$_{ipso}$), 139.66 (Xanth-*C*^{11}), 130.11 (Xanth-*C*^{10}), 122.09 (Ar-*C*H), 109.81 (Xanth-*C*^{3}H), 108.53 (Xanth-*C*^{1}H), 42.37 (Zr(N*Me$_2$*)$_2$), 35.56 (Xanth-*C*^{9}Me$_2$), 35.10 (*C*Me$_3$), 34.57 (para-*C*HMe$_2$), 31.87 (C*Me$_3$*), 30.23 (C*Me$_2$*), 28.55 (ortho-*C*HMe$_2$), 26.01 (B-ortho-CH*Me$_2$*), 24.79 (A-ortho-CH*Me$_2$*), 24.41 (para-CH*Me$_2$*). **Anal. Calcd. For C$_{60}$H$_{95}$N$_4$O$_{1.5}$SiZr:** C, 70.95; H, 9.42; N, 5.51 %. Found: C, 70.99; H, 9.23; N, 5.47 %.

[(XN$_2$ZrMe$_2$] (2): [(XN$_2$)Zr(NMe$_2$)$_2$]·(O(SiMe$_3$)$_2$)$_{0.5}$ (**1**) (0.095 g, 0.093 mmol) was dissolved in 2 mL of benzene, to which AlMe$_3$ (0.067 g, 0.935 mmol) was added and the solution was stirred at 24 °C in a sealed Schlenk flask for 7 days. The solvent was removed *in vacuo* and the yellow solid was recrystalized from a concentrated pentane solution cooled to –30 °C, yielding yellow crystals of **2** (0.051 g, 62 %). **^{1}H NMR (C$_6$D$_6$, 600 MHz):** δ 7.33 (s, 4H, Ar-*H*), 6.84 (d, 2H, $^4J_{H,H}$ 1.84 Hz, Xanth-C*H*^{1}), 6.24 (d, 2H, $^4J_{H,H}$ 1.87 Hz, Xanth-C*H*^{3}), 3.72 (sept, 4H, $^3J_{H,H}$ 6.72 Hz, ortho-C*H*Me$_2$), 2.85 (sept, 2H, $^3J_{H,H}$ 6.89 Hz, para-C*H*Me$_2$), 1.47 (s, 6H, C*Me$_2$*), 1.43 (d, 12H, $^3J_{H,H}$ 6.88 Hz, A-ortho-CH*Me$_2$*), 1.23 (d, 12H, $^3J_{H,H}$ 6.87 Hz, para-CH*Me$_2$*), 1.22 (s, 18H, C*Me$_3$*), 1.20 (d, 12H, $^3J_{H,H}$ 6.70 Hz, B-ortho-CH*Me$_2$*), 0.78 (s, 6H, Zr*Me$_2$*). **^{13}C NMR (C$_6$D$_6$, 126 MHz):** δ 148.48 (Xanth-*C*^{2}), 148.02 (para-*C*CHMe$_2$), 146.88 (ortho-*C*CHMe$_2$), 145.86 (Xanth-*C*^{4}), 140.28 (Xanth-*C*^{11}), 137.01 (Ar-*C*$_{ipso}$), 128.94 (Xanth-*C*^{10}), 122.84 (Ar-*C*H), 110.90 (Xanth-*C*^{1}H), 109.79 (Xanth-*C*^{3}H), 50.02 (Zr*Me$_2$*), 35.10 (*C*Me$_3$), 35.09 (Xanth-*C*^{9}Me$_2$), 34.50 (para-*C*HMe$_2$), 31.70 (C*Me$_3$*), 31.42 (C*Me$_2$*), 29.01 (ortho-*C*HMe$_2$), 26.86 (B-ortho-CH*Me$_2$*), 24.68 (A-ortho-CH*Me$_2$*), 24.24 (para-CH*Me$_2$*). **Anal. Calcd. For C$_{55}$H$_{80}$N$_2$OZr:** C, 75.37; H, 9.20; N, 3.19 %. Found: C, 75.03; H, 8.88; N, 3.08 %.

[(XN$_2$)ZrCl$_2$] (3): [(XN$_2$)Zr(NMe$_2$)$_2$]·(O(SiMe$_3$)$_2$)$_{0.5}$ (**1**) (0.15 g, 0.147 mmol) was dissolved in 6 mL of benzene, to which Me$_3$SiCl (0.04 g, 0.369 mmol) was added and the solution was stirred at 24 °C in a sealed Schlenk flask for 14 days. The solvent was removed *in vacuo* and the yellow solid was recrystalized from a concentrated pentane solution cooled to –30 °C yielding **3** as a bright yellow powder (0.086 g, 64 %). **^{1}H NMR (C$_6$D$_6$, 600 MHz):** δ 7.29 (s, 4H, Ar-*H*), 6.89 (d, 2H, $^4J_{H,H}$ 1.96 Hz, Xanth-C*H*'), 6.22 (d, 2H, $^4J_{H,H}$ 1.96 Hz, Xanth-C*H*''), 3.67 (sept, 4H, $^3J_{H,H}$ 6.68 Hz, ortho-C*H*Me$_2$), 2.79 (sept, 2H, $^3J_{H,H}$ 6.86 Hz, para-C*H*Me$_2$), 1.56 (d, 12H, $^3J_{H,H}$ 6.80 Hz, A-ortho-CH*Me$_2$*), 1.35 (s, 6H, C*Me$_2$*), 1.18 (s, 18H, C*Me$_3$*), 1.17 (d, 12H, $^3J_{H,H}$ 6.86 Hz, para-CH*Me$_2$*), 1.14 (d, 12H, $^3J_{H,H}$ 6.72 Hz, B-ortho-CH*Me$_2$*). **^{13}C NMR (C$_6$D$_6$, 126 MHz):** δ 149.46 (Xanth-*C*^{2}), 149.07 (para-*C*CHMe$_2$), 146.08 (ortho-*C*CHMe$_2$), 136.75 (Ar-*C*$_{ipso}$), 130.21 (Xanth-*C*^{10}), 123.15 (Ar-*C*H), 112.43 (Xanth-*C*H'), 109.77 (Xanth-*C*H''), 35.58 (Xanth-*C*^{9}Me$_2$), 35.17 (*C*Me$_3$), 34.43 (para-*C*HMe$_2$), 31.64 (C*Me$_3$*), 30.09 (C*Me$_2$*), 29.24 (ortho-*C*HMe$_2$), 26.58 (B-ortho-CH*Me$_2$*), 24.90 (A-ortho-CH*Me$_2$*), 24.11 (para-CH*Me$_2$*). **Anal. Calcd. For C$_{53}$H$_{74}$N$_2$OZrCl$_2$:** C, 69.39; H, 8.13; N, 3.05 %. Found: C, 68.89; H, 8.02; N, 3.44 %.

[(XN$_2$)ZrMe][MeB(C$_6$F$_5$)$_3$] (4): [(XN$_2$ZrMe$_2$] (**2**) (0.075 g, 0.085 mmol) was dissolved in 1.5 mL of toluene, to which B(C$_6$F$_5$)$_3$ (0.044 g, 0.085 mmol) was added and the solution was stirred at 24 °C for 5 min. The toluene solution was then layered with pentane (5 mL) and cooled to –30 °C, which yielded bright yellow crystals of **4** (0.091 g, 77 %). **^{1}H NMR (C$_6$D$_6$, 600 MHz):** δ 7.24 (d, 2H, $^4J_{H,H}$ 1.8 Hz, Ar-*H*'), 7.20 (d, 2H, $^4J_{H,H}$ 1.7 Hz, Ar-*H*''), 6.92 (d, 2H, $^4J_{H,H}$ 1.8 Hz, Xanth-C*H*'), 6.15 (br. s, 2H, Xanth-C*H*''), 3.48 (br. sept, 2H, A-ortho-C*H*Me$_2$), 2.71 (sept, 2H, $^3J_{H,H}$ 6.8 Hz, para-C*H*Me$_2$), 2.67 (sept, 2H, $^3J_{H,H}$ 6.8 Hz, B-ortho-C*H*Me$_2$), 1.87 (br. s, 3H, Zr-*Me*), 1.80 (br. s, 3H, B-*Me*), 1.55 (d, 6H, $^3J_{H,H}$ 6.1 Hz, A-ortho-CH*Me$_2$*'), 1.35 (s, 3H, C*Me$_2$*'), 1.30 (s, 3H, C*Me$_2$*''), 1.11 (s, 18H, C*Me$_3$*), 1.09 (d, 12H, $^3J_{H,H}$ 6.8 Hz, para-CH*Me$_2$*), 1.06 (d, 6H, $^3J_{H,H}$ 6.6 Hz, A-ortho-CH*Me$_2$*''), 0.91 (d, 6H, $^3J_{H,H}$ 6.5 Hz, B-ortho-CH*Me$_2$*'), 0.68 (br. d, 6H, B-ortho-CH*Me$_2$*''). **^{13}C NMR (C$_6$D$_6$, 126 MHz):** δ 151.45 (Xanth-*C*^{2}), 150.03 (para-*C*CHMe$_2$), 148.38 (**A**-ortho-*C*CHMe$_2$), 144.60 (B-ortho-*C*CHMe$_2$), 141.74 (Xanth-*C*^{11}), 130.96 (Ar-*C*$_{ipso}$), 130.15 (Xanth-*C*^{10}), 125.15 (Ar-*C*H'), 123.64 (Ar-*C*H''), 113.86 (Xanth-*C*H'), 110.08 (Xanth-*C*'H''), 55.56 (Zr-*Me*), 35.50 (Xanth-*C*^{9}Me$_2$), 35.34 (*C*Me$_3$), 35.20 (br., B-*Me*), 35.18 (C*Me$_2$*''), 34.28 (para-*C*HMe$_2$), 31.49 (C*Me$_3$*), 30.59 (B-ortho-*C*HMe$_2$), 28.64 (A-ortho-*C*HMe$_2$), 26.98 (A-ortho-CH*Me$_2$*''), 26.40 (B-ortho-CH*Me$_2$*'), 24.82 (C*Me$_2$*'), 24.13 (A-ortho-CH*Me$_2$*'), 23.51 (para-CH*Me$_2$*), 23.05 (B-ortho-CH*Me$_2$*''). **^{19}F NMR (C$_6$D$_6$, 188 MHz):** δ –129.1 (d, $^3J_{F,F}$ 21.8 Hz, *o*-C$_6$F$_5$), –158.67 (t, $^3J_{F,F}$ 20.6 Hz, *p*-C$_6$F$_5$), -162.26 (br. t, *m*-C$_6$F$_5$). **Anal. Calcd. For C$_{73}$H$_{80}$N$_2$OZrBF$_{15}$:** C, 63.15; H, 5.80; N, 2.02 %. Found: C, 63.67; H, 6.00; N, 2.12 %.

[(XN$_2$)ZrMe(η^6-toluene)][B(C$_6$F$_5$)$_4$] (5b): [(XN$_2$ZrMe$_2$] (**2**) (0.075 g, 0.085 mmol) was dissolved in 1.5 mL of toluene, to which [CPh$_3$][B(C$_6$F$_5$)$_4$] (0.080 g, 0.085 mmol) was added and the solution was stirred at 24 °C for 5 min. The toluene solution was then layered with pentane (5 mL) and cooled to –30 °C, which yielded bright red crystals of [(XN$_2$)ZrMe(η^6-toluene)][B(C$_6$F$_5$)$_4$] (0.118 g, 84 %). **^{1}H NMR (C$_6$D$_6$, 600 MHz, 300K):** identical to that of **5a** in C$_6$D$_6$, but containing free toluene. Selected additional NMR data: **^{1}H NMR (d$_8$-Tol, 600 MHz, 300K):** δ 0.84 (s, 3H, Zr-*Me*). **^{1}H NMR (C$_6$D$_5$Br, 500 MHz, 248 K)** δ 7.26 (m, 1H, Coord. Toluene C*H*-*p*), 6.97 (s, 2H, Xanth-C*H*''), 6.80 (d, 2H, $^3J_{H,H}$ 7 Hz, Coord. Toluene C*H*-*o*), 6.21 (t, 2H, $^3J_{H,H}$ 7 Hz, Coord. Toluene C*H*-*m*), 5.71 (s, 2H, Xanth-C*H*'), 2.23 (s, 3H, Coord. Toluene C*H$_3$*). **Anal. Calcd. For C$_{85}$H$_{85}$N$_2$OZrBF$_{20}$:** C, 62.53; H, 5.25; N, 1.71 %. Found: C, 59.29; H, 5.10; N, 1.77 %. Crystals of this compound rapidly decomposed to multiple unidentified products when the supernatant was removed, so a successful elemental analysis was not obtained.

In-situ generated [(XN$_2$)ZrMe(arene)][B(C$_6$F$_5$)$_4$] {arene = η^6-benzene (5a) and bromobenzene (5c)}: Compound **2** (0.075 g, 0.085 mmol) was dissolved in 1.5 mL of benzene or bromobenzene, to which [CPh$_3$][B(C$_6$F$_5$)$_4$] (0.080 g, 0.085 mmol) was added and the solution was stirred at 24 °C for 5 min. **^{1}H NMR for 5a (C$_6$D$_6$, 600 MHz)):** δ 7.28 (br. s, 2H, Ar-*H*'), 7.27 (br. s, 2H, Ar-*H*''), 6.90 (d, 2H, $^4J_{H,H}$ 1.7 Hz, Xanth-C*H*'), 5.84 (d, 2H, $^4J_{H,H}$ 1.9 Hz, Xanth-C*H*''), 2.93 (sept, 2H, $^3J_{H,H}$ 6.8 Hz, para-C*H*Me$_2$), 2.85 (sept, 2H, $^3J_{H,H}$ 6.9 Hz, A-ortho-C*H*Me$_2$), 2.80 (sept, 2H, $^3J_{H,H}$ 6.8 Hz, B-ortho-C*H*Me$_2$), 1.34 (s, 3H, C*Me$_2$*'), 1.32 (s, 3H, C*Me$_2$*''), 1.31 (d, 6H, $^3J_{H,H}$ 6.9 Hz, A-ortho-CH*Me$_2$*'), 1.30 (d, 12H, $^3J_{H,H}$ 6.9 Hz, para-CH*Me$_2$*), 1.28 (d, 6H, $^3J_{H,H}$ 6.9 Hz, B-ortho-CH*Me$_2$*'), 1.09 (s, 18H, C*Me$_3$*), 0.99 (d, 6H, $^3J_{H,H}$ 6.8 Hz, A-ortho-CH*Me$_2$*''), 0.91 (s, 3H, Zr-*Me*), 0.81 (d, 6H, $^3J_{H,H}$ 6.8 Hz, B-ortho-CH*Me$_2$*''). **^{13}C NMR (C$_6$D$_6$, 126 MHz):** δ 150.57 (para-*C*CHMe$_2$), 149.30 (Xanth-*C*^{2}), 145.79 (Ar-*C*$_{ipso}$), 145.12

(A-ortho-*C*CHMe$_2$), 142.78 (B-ortho-*C*CHMe$_2$), 141.15 (Xanth-*C*^{11}), 130.17 (Xanth-*C*^{10}), 123.61 (Ar-*C*H'), 122.98 (Ar-*C*H''), 114.13 (Xanth-*C*H'), 111.53 (Xanth-*C*H''), 43.53 (Zr-*Me*), 36.36 (C*Me$_2$*''), 35.07 (*C*Me$_3$), 35.01 (Xanth-*C*^{9}Me$_2$), 34.57 (para-*C*HMe$_2$), 31.29 (C*Me$_3$*), 30.05 (B-ortho-*C*HMe$_2$), 28.23 (A-ortho-*C*HMe$_2$), 26.53 (B-ortho-CH*Me$_2$*''), 26.43 (A-ortho-CH*Me$_2$*''), 24.37 (C*Me$_2$*'), 23.98 (para-CH*Me$_2$*), 23.66 (A-ortho-CH*Me$_2$*'), 23.32 (B-ortho-CH*Me$_2$*'). **^{19}F NMR (C_6D_6, 188 MHz):** δ –130.02 (br. d, *o*-C_6F_5), –160.67 (t, $^3J_{F,F}$ 22.2 Hz, *p*-C_6F_5), –164.46 (br. t, $^3J_{F,F}$ 18.8 Hz, *m*-C_6F_5). Selected NMR data for **5c**: **^{1}H NMR for 5c (C_6D_5Br, 500 MHz, 300 K):** δ 6.13 (br. s, 2H, Xanth-C*H*'). **^{1}H NMR for 5c (C_6D_5Br, 500 MHz, 248 K):** δ 7.06 (br. s, 1.3H, Isomer A Xanth-C*H*''), 6.98 (br. s, 0.7H, Isomer B Xanth-C*H*''), 6.23 (s, 1.3H, Isomer A Xanth-C*H*'), 5.80 (s, 0.7H, Isomer B Xanth-C*H*').

General Procedure for Intramolecular Hydroamination In the glove box, a d_8-toluene solution of **2**; or a C_6D_6 solution of [(XN_2)ZrMe$_2$] with 1 added equivalent of either B(C_6F_5)$_3$ or [CPh$_3$][B(C_6F_5)$_4$], was prepared and added to the hydroamination substrate (dissolved in C_6D_6 or d_8-toluene), and placed in a teflon-valved J-young NMR tube. The reactions were monitored at 24 °C or 110 °C by ^{1}H NMR spectroscopy and organic products were identified by comparison with reported literature spectra.[38]

General Procedure for Ethylene Polymerization: In the glove box, 5 mg (0.0057 mmol) of [(XN_2)ZrMe$_2$] was dissolved in approx. 4.75 mL (approx. 1.2 mM) of toluene or bromobenzene, 1 equivalent of either B(C_6F_5)$_3$ or [CPh$_3$][B(C_6F_5)$_4$] was added, and the solution was allowed to react for 5 min at 24 °C. The solution was briefly evacuated before placing the flask under dynamic ethylene (1 atm) and the solution was allowed to react for the designated period of time. In the case of high temperature polymerization, the solution was placed in a preheated oil bath (80 °C) before opening to ethylene. After the specified period of time, the solution was opened to air and acidified methanol (10 % HCl) was added. The polyethylene solid was filtered, washed with methanol and acetone and then dried in a 40 °C oven and weighed to obtain the yield.

ASSOCIATED CONTENT

Supporting Information

NMR spectra for new compounds and hydroamination reactions, and GPC data is included in the Supporting Information, which is available free of charge on the ACS Publications website. CCDC 1554817-1554820 contain the supplementary crystallographic data for **1**, **2**, **4** and **5b**, respectively. These data can be obtained free of charge from The Cambridge Crystallographic Data Centre via www.ccdc.cam.ac.uk/data_request/cif.

AUTHOR INFORMATION

Corresponding Author

* D.J.H.E.: tel, 905-525-9140; fax, 905-522-5209;
e-mail: emslied@mcmaster.ca.

Notes

The authors declare no competing financial interests.

ACKNOWLEDGMENT

D.J.H.E. thanks NSERC of Canada for a Discovery Grant. K.S.A.M. thanks the Government of Ontario for an OGS - Queen Elizabeth II Graduate Scholarship in Science and Technology (QEII GSST) scholarship. We are grateful to N. R. Andreychuk of the Emslie group for DSC measurements.

REFERENCES

(1) a) Coates, G. W. *Chem. Rev.* **2000**, *100*, 1223. b) Alt, H. G.; Köppl, A. *Chem. Rev.* **2000**, *100*, 1205. c) McKnight, A. L.; Waymouth, R. M. *Chem. Rev.* **1998**, *98*, 2587. d) Gibson, V. C.; Spitzmesser, S. K. *Chem. Rev.* **2003**, *103*, 283. e) Collins, R. A.; Russell, A. F.; Mountford, P. *Appl. Petrochem. Res.* **2015**, *5*, 153.

(2) Chen, E. Y.-X.; Marks, T. J. *Chem. Rev.* **2000**, *100*, 1391.

(3) Matsui, S.; Mitani, M.; Saito, J.; Tohi, Y.; Makio, H.; Matsukawa, N.; Takagi, Y.; Tsuru, K.; Nitabaru, M.; Nakano, T.; Tanaka, H.; Kashiwa, N.; Fujita, T. *J. Am. Chem. Soc.* **2001**, *123*, 6847.

(4) a) Hayes, P. G.; Piers, W. E.; Parvez, M. *J. Am. Chem. Soc.* **2003**, *125*, 5622. b) Hayes, P. G.; Piers, W. E.; Parvez, M. *Chem. Eur. J.* **2007**, *13*, 2632.

(5) Cruz, C. A.; Emslie, D. J. H.; Robertson, C. M.; Harrington, L. E.; Jenkins, H. A.; Britten, J. F. *Organometallics* **2009**, *28*, 1891.

(6) Lancaster, S. J.; Robinson, O. B.; Bochmann, M.; Coles, S. J.; Hursthouse, M. B. *Organometallics* **1995**, *14*, 2456.

(7) Gillis, D. J.; Quyoum, R.; Tudoret, M.-J.; Wang, Q.; Jeremic, D.; Roszak, A. W.; Baird, M. C. *Organometallics* **1996**, *15*, 3600.

(8) Altaf, A. A.; Badshah, A.; Khan, N.; Marwat, S.; Ali, S. *J. Coord. Chem.* **2011**, *64*, 1815.

(9) a) Scollard, J. D.; McConville, D. H.; Payne, N. C.; Vittal, J. J. *Macromolecules* **1996**, *29*, 5241. b) Scollard, J. D.; McConville, D. H. *J. Am. Chem. Soc.* **1996**, *118*, 10008.

(10) Chen, Y.-X.; Marks, T. J. *Organometallics* **1997**, *16*, 3649.

(11) a) Gillis, D. J.; Tudoret, M.-J.; Baird, M. C. *J. Am. Chem. Soc.* **1993**, *115*, 2543. b) Wang, Q.; Quyoum, R.; Gillis, D. J.; Tudoret, M.-J.; Jeremic, D.; Hunter, B. K.; Baird, M. C. *Organometallics* **1996**, *15*, 693.

(12) Cruz, C. A.; Emslie, D. J. H.; Harrington, L. E.; Britten, J. F.; Robertson, C. M. *Organometallics* **2007**, *26*, 692.

(13) Cruz, C. A.; Emslie, D. J. H.; Harrington, L. E.; Britten, J. F. *Organometallics* **2008**, *27*, 15.

(14) Andreychuk, N. R.; Ilango, S.; Vidjayacoumar, B.; Emslie, D. J. H.; Jenkins, H. A. *Organometallics* **2013**, *32*, 1466.

(15) Motolko, K. S. A.; Emslie, D. J. H.; Jenkins, H. A. *Organometallics* **2017**, *36*, 1601.

(16) Motolko, K. S. A.; Emslie, D. J. H.; Britten, J. F. *RSC Advances* **2017**, *7*, 27938.

(17) For the synthesis of *N*-mesityl and *N*-cyclohexyl substituted 4,5-bis(amido)xanthene ligands, and the preparation of titanium(IV) bis(amido) and dibenzyl complexes, see: Porter, R. M.; Danopoulos, A. A. *Polyhedron* **2006**, *25*, 859.

(18) a) Menard, G.; Jong, H.; Fryzuk, M. D. *Organometallics* **2009**, *28*, 5253. b) Zhu, T.; Wambach, T. C.; Fryzuk, M. D. *Inorg. Chem.* **2011**, *50*, 11212.

(19) Batke, S.; Sietzen, M.; Merz, L.; Wadepohl, H.; Ballmann, J. *Organometallics* **2016**, *35*, 2294.

(20) Tonks, I. A.; Tofan, D.; Weintrob, E. C.; Agapie, T.; Bercaw, J. E. *Organometallics* **2012**, *31*, 1965.

(21) O'Shaughnessy, P. N.; Gillespie, K. M.; Morton, C.; Westmoreland, I.; Scott, P. *Organometallics* **2002**, *21*, 4496.

(22) a) Cortright, S. B.; Huffman, J. C.; Yoder, R. A.; Coalter, J. N.; Johnston, J. N. *Organometallics* **2004**, *23*, 2238. b) Riley, P. N.; Fanwick, P. E.; Rothwell, I. P. *J. Chem. Soc. Dalton Trans.* **2001**, 181.

(23) Thermal decomposition of dimethyl compound **2,** and monoalkyl cations **4** and **5** led to a mixture of unidentified products, with release of methane.

(24) Schrock, R. R.; Baumann, R.; Reid, S. M.; Goodman, J. T.; Stumpf, R.; Davis, W. M. *Organometallics* **1999**, *18*, 3649.

(25) Schrock, R. R.; Casado, A. L.; Goodman, J. T.; Liang, L. C.; Bonitatebus, P. J.; Davis, W. M. *Organometallics* **2000**, *19*, 5325.

(26) a) Mehrkhodavandi, P.; Schrock, R. R.; Bonitatebus, P. J. *Organometallics* **2002**, *21*, 5785. b) Schrock, R. R.; Schattenmann, F.; Aizenberg, M.; Davis, W. M. *Chem. Commun.* **1998**, 199. c) Baumann, R.; Stumpf, R.; Davis, W. M.; Liang, L. C.; Schrock, R. R. *J.*

Am. Chem. Soc. **1999**, *121*, 7822. d) Flores, M. A.; Manzoni, M. R.; Baumann, R.; Davis, W. M.; Schrock, R. R. *Organometallics* **1999**, *18*, 3220. e) Lee, C. S.; Park, J. H.; Hwang, E. Y.; Park, G. H.; Go, M. J.; Lee, J.; Lee, B. Y. *J. Organomet. Chem.* **2014**, *772*, 172. f) Tonzetich, Z. J.; Lu, C. C.; Schrock, R. R.; Hock, A. S.; Bonitatebus, P. J. *Organometallics* **2004**, *23*, 4362.

(27) Lee, C. H.; La, Y. H.; Park, J. W. *Organometallics* **2000**, *19*, 344.

(28) Horton, A. D.; de With, J.; van der Linden, A. J.; van de Weg, H. *Organometallics* **1996**, *15*, 2672.

(29) a) Yang, X.; Stern, C. L.; Marks, T. J. *J. Am. Chem. Soc.* **1991**, *113*, 3623. b) Bochmann, M.; Lancaster, S. J.; Hursthouse, M. B.; Malik, K. M. A. *Organometallics* **1994**, *13*, 2235. c) Gómez, R.; Green, M. L. H.; Haggitt, J. L. *J. Chem. Soc. Dalton Trans.* **1996**, 939. d) Beck, S.; Prosenc, M. H.; Brintzinger, H. H.; Goretzki, R.; Herfert, N.; Fink, G. *J. Mol. Catal. A: Chem.* **1996**, *111*, 67. e) Bazan, G. C.; Cotter, W. D.; Komon, Z. J. A.; Lee, R. A.; Lachicotte, R. J. *J. Am. Chem. Soc.* **2000**, *122*, 1371. f) Beck, S.; Lieber, S.; Schaper, F.; Geyer, A.; Brintzinger, H. H. *J. Am. Chem. Soc.* **2001**, *123*, 1483. g) Liu, Z. X.; Somsook, E.; Landis, C. R. *J. Am. Chem. Soc.* **2001**, *123*, 2915. h) Chen, M. C.; Roberts, J. A. S.; Marks, T. J. *J. Am. Chem. Soc.* **2004**, *126*, 4605. i) Li, H. B.; Li, L. T.; Schwartz, D. J.; Metz, M. V.; Marks, T. J.; Liable-Sands, L.; Rheingold, A. L. *J. Am. Chem. Soc.* **2005**, *127*, 14756. j) Al-Humydi, A.; Garrison, J. C.; Mohammed, M.; Youngs, W. J.; Collins, S. *Polyhedron* **2005**, *24*, 1234. k) Yang, X.; Stern, C. L.; Marks, T. J. *J. Am. Chem. Soc.* **1994**, *116*, 10015.

(30) Baumann, R.; Davis, W. M.; Schrock, R. R. *J. Am. Chem. Soc.* **1997**, *119*, 3830.

(31) a) Bondi, A. *J. Phys. Chem.* **1964**, *68*, 441. b) Batsanov, S. S. *Inorg. Mater.* **2001**, *37*, 871. c) Mantina, M.; Chamberlin, A. C.; Valero, R.; Cramer, C. J.; Truhlar, D. G. *J. Phys. Chem. A* **2009**, *113*, 5806. d) Nag, S.; Banerjee, K.; Datta, D. *New J. Chem.* **2007**, *31*, 832. Alvarez, S. *Dalton Trans.* **2013**, *42*, 8617.

(32) Shannon, R. D. *Acta Cryst.* **1976**, *A32*, 751.

(33) For examples of chlorobenzene or fluorobenzene κ^1-coordinated to group 3 or 4 transition metals, see: a) Bouwkamp, M. W.; de Wolf, J.; Morales, I. D.; Gercama, J.; Meetsma, A.; Troyanov, S. I.; Hessen, B.; Teuben, J. H. *J. Am. Chem. Soc.* **2002**, *124*, 12956. b) Bouwkamp, M. W.; Budzelaar, P. H. M.; Gercama, J.; Del Hierro Morales, I.; de Wolf, J. M., A.; Troyanov, S. I.; Teuben, J. H.; Hessen, B. *J. Am. Chem. Soc.* **2005**, *127*, 14310. c) Basuli, F.; Aneetha, H.; Huffman, J. C.; Mindiola, D. J. *J. Am. Chem. Soc.* **2005**, *127*, 17992. d) Chapman, A. M.; Haddow, M. F.; Wass, D. F. *J. Am. Chem. Soc.* **2011**, *133*, 18463. e) Metters, O. J.; Forrest, S. J. K.; Sparkes, H. A.; Manners, I.; Wass, D. F. *J. Am. Chem. Soc.* **2016**, *138*, 1994.

(34) Jeon, Y. M.; Park, S. J.; Heo, J.; Kim, K. *Organometallics* **1998**, *17*, 3161.

(35) Li, G.; Zuccaccia, C.; Tedesco, C.; D'Auria, I.; Macchioni, A.; Pellecchia, C. *Chem. Eur. J.* **2014**, *20*, 232.

(36) Michiue, K.; Jordan, R. F. *J. Mol. Catal. A: Chem.* **2008**, *282*, 107.

(37) Burger, B. J.; Bercaw J. E. *Vacuum Line Techniques for Handling Air-Sensitive Organometallic Compounds*. In *Experimental Organometallic Chemistry: A Practicum in Synthesis and Characterization*; Wayda, A. L., Darensbourg, M. Y., Eds.; ACS Symp. Ser.; American Chemical Society: Washington D.C., 1987, Vol. 357, pp 79-98.

(38) Crimmin, M. R.; Arrowsmith, M.; Barrett, A. G. M.; Casely, I. J.; Hill, M. S.; Procopiou, P. A. *J. Am. Chem. Soc.* **2009**, *131*, 9670.

(39) Pohlmann, J. L. W.; Brinckmann, F. E. *Z. Naturforsch. B* **1965**, *20*, 5.

Authors are required to submit a graphic entry for the Table of Contents (TOC) that, in conjunction with the manuscript title, should give the reader a representative idea of one of the following: A key structure, reaction, equation, concept, or theorem, etc., that is discussed in the manuscript. Consult the journal's Instructions for Authors for TOC graphic specifications.

Insert Table of Contents artwork here